Chapter

Quantitative Imaging Parameters in the Diagnosis of Endometriomas

Paul-Andrei Ștefan, Roxana-Adelina Lupean and Dietmar Tamandl

Abstract

The classic imaging diagnosis of endometriomas encounters multiple limitations, including the subjective evaluation of medical examinations and a similar imaging appearance with other adnexal lesions, especially the functional hemorrhagic cysts. For this reason, a definite diagnosis of endometriomas can be made only by pathological analysis, which reveals particular features in terms of cellularity and biochemical components of their fluid content. It is theorized that these histopathological features can also be reflected in medical images, altering the pixel intensity and distribution, but these changes are too subtle to be assessed by the naked eye. New quantitative imaging evaluations and emerging computer-aided diagnosis techniques can provide a detailed description of image contents that can be furtherly processed by algorithms, aiming to provide a more accurate and non-invasive diagnosis for this disease.

Keywords: computer-aided diagnosis, endometrioma, endometriosis, MRI, texture analysis

1. Introduction

Laparoscopic biopsy of suspicious-looking lesions, followed by histologic confirmation, is the gold standard for diagnosing pelvic endometriosis [1]. The first line imaging of ovarian endometriotic lesions (endometriomas) remains transvaginal ultrasonography (TVUS) which is able, in most situations, to offer sufficient information for adequate preoperative planning [2]. Other diagnostic procedures, such as magnetic resonance imaging (MRI), are used in certain circumstances based on the results of the TVUS and the severity of the symptoms. The pelvic MRI scan provides for full lesion mapping, with a high detection rate for both anterior and, particularly, posterior lesions, whereas TVUS shows lower sensitivity rates [3]. MRI shows higher accuracy for the detection and characterization of endometriotic lesions than other imaging modalities, therefore it is often used to evaluate adnexal masses and monitor treatment response, potentially avoiding the need for a follow-up laparoscopy [4]. Moreover, this method is especially usefull in the detection of deep infiltrating

endometriosis, being absolutely required in this subcohort of patients. As with any other imaging modality, the MRI evaluation of endometriosis is limited by the technique itself, but more by the examiner's experience and level of training, since all classic MRI signs of this disease are qualitative and entire subjectively evaluated.

One of the most challenging tasks in the diagnosis of endometriomas is distinguishing these lesions from functional hemorrhagic ovarian cysts (HCs) since they share many both imaging and histological characteristics. To avoid unnecessary surgery, it's critical to correctly distinguish the two lesions [5]. As a result, the difference in imaging between the two entities has a significant impact on the subsequent medical and surgical treatment options [6]. This chapter focuses on the emerging quantitative imaging modalities that can improve the diagnostic and characterization of endometriomas and may aid to distinguish these lesions from HCs.

2. MRI signal intensity measurements

The "T2 shading" sign is currently considered a characteristic MRI finding of endometriomas [7]. This sign refers to a cystic lesion with a high signal on T1-weighted (T1W) sequences and subsequent T2 shortening which results in hypointensity on T2-weighted (T2W) images, as a result of in-lesion hemorrhage and accumulation of blood products and proteins [8, 9].

The "T2 shading" was first described by Togashi and colleagues [10] in 1991, who attributed it high diagnostic value (98% sensitivity and 96% specificity). Following further investigation, more recent studies demonstrated that this sign is not as specific to endometriomas as originally thought, mostly due to the subjective character of the imaging findings [11] and the occurrence of this sign in other ovarian cysts accompanied by bleeding [12–14]. The acknowledgment of these limitations drastically decreased the utility of this sign in further studies (with a sensitivity and specifity as low as 68% and sensitivity and 14.2%, respectively specificity) [11, 12].

It is important to remember that some HCs have a delayed regression and may accumulate blood products, which also leads to a decrease in their intrinsec signal on T2W sequences [14]. However, it is expected that HCs would accumulate f blood products to a lesser degree compared to endometriomas, since they usually regress within a few menstrual cycles and do not exhibit cyclic intra-lesional bleeding. In this regard, Outwater et al. [11] concluded that endometriomas tend to

Author	Year	Sensitivity	Specificity
Dias et al. [15]	2015	73%	93%
Lee et al. [12]	2015	89.8%	14.2%
Outwater et al. [11]	1993	68%	76%
Sugimura et al. [16]	1993	82%	91%
Sugimura et al. [16]	1993	11%	98%
Scout et al. [17]	1994	92%	91%

Table 1.
The diagnostic ability of the "T2 shading" sign for identifying endometriomas.

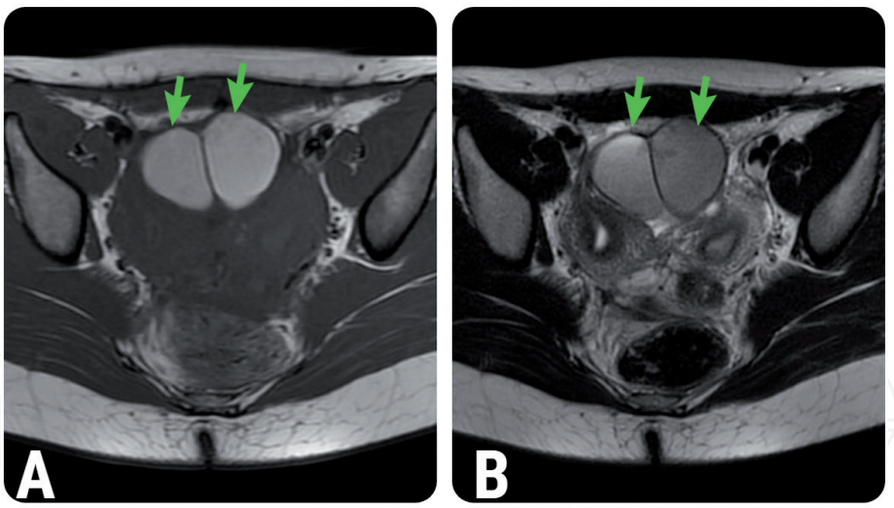

Figure 1.
The magnetic resonance (MRI) representation of the "T2 shading" sign, based on the examination of a patient with two histologically-proven endometriotic lesions. (A) On the axial T1-weighted image, both lesions express similar high-signal intensity (green arrows). (B) On the T2-weighted image, the two lesions express different degrees of signal drop (green arrows).

have higher T1 and lower T2 signal intensities (SI) than HCs, thus creating a more abrupt "shading" phenomenon. However, previous studies did not provide a clear definition of the extent of the signal difference between T1W and T2W sequences, and the degree required for this in order to become a confident diagnostic criterion (**Table 1**). An adequate example of the variation of this signs' appearance is demonstrated in **Figure 1**.

Lately, a small-cohort study [18] aimed to differentiate endometriomas from HCs by quantifying the "T2 shading" sign through signal intensity (SI) measurements made by placing regions of interest (ROIs) within the lesions on T1 and T2 weighted-images (WI). The signal intensity difference was quantified by subtracting SI values between T1 and T2 WI (A = T1 – T2). There were statistically significant differences between the two entities only when comparing T1 SIs ($p = 0.0003$) due to the much higher values obtained by endometriomas, while the T2 SIs were very similar and did not differ significantly ($p = 0.27$). As expected, endometriomas demonstrated a higher loss (median SI loss = 432.95 units) while HCs recorded negative results (median SI loss = −46.8 units). In most cases, the values recorded by HCs on T2 WI were higher than the ones on T1 WI, which could be a consequence of the HCs' blood content being in different stages of degradation and to an overall lesser amount of blood products or protein accumulation (or to a higher percentage of intrinsically present fluid – which is usually not present in endometriomas). These results are in accordance with the early observations of Outwater et al. [11] that were mentioned earlier.

Through the quantitative appreciation of the "shading" sign, using a cut-off for the signal drop of more than 31.3 SI units, endometriomas could be differentiated from HCs with 100% sensitivity and 81.82% specificity. Therefore, this study [18] concluded that the key in identifying endometriomas relies upon a brighter T1 appearance of the lesions, which cannot be always appreciated by the visual evaluation (**Figure 2**). As the proposed measurement technique is rather basic, it could be easily translated into daily clinical practice, possible offering more confidence in the MRI diagnosis of these lesions.

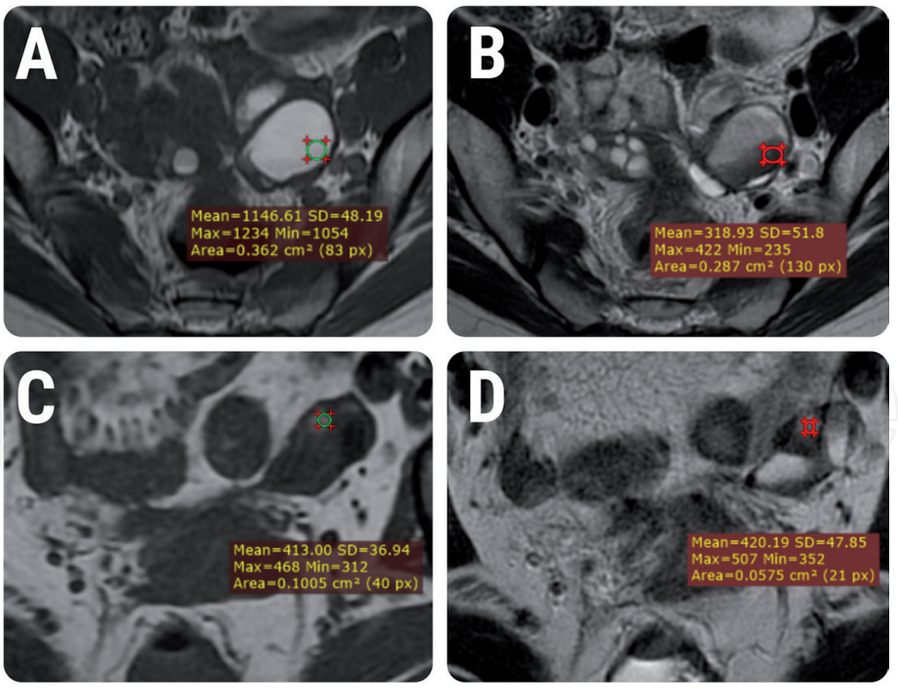

Figure 2.
Quantitative assessment of the "T2 shading" sign in endometriomas and functional hemorrhagic cysts. (A and B) The MRI examination of a 32-year old patient with endometrioma. The difference in signal intensity between (A) T1 (1146.61 units) and (B) T2 (318.93 units) was 827.68 units. (C and D) The MRI examination of a 27-year old patient with an ovarian hemorrhagic cyst. The difference in signal intensity between (C) T1 (413 units) and (D) T2 (420.19 units) was −7.19 units.

3. Diffusion-weighted imaging

MRI incorporates a functional technique known as diffusion-weighted imaging (DWI). DWI sequences provide information about the Brownian motion of water molecules in a tissue [19]. Based on these sequences, apparent diffusion coefficient (ADC) maps can be computed, and together they offer qualitative and quantitative information about tissue density [20]. Tissues that are highly cellular or have cellular swelling show lower water diffusion coefficients which translate to higher SI on DWI sequences and lower values on ADC maps. The ADC value can be quantified as SI values through ROI placement, and can also be used as a marker of cellularity [20]. In recent years, these sequences have evolved as a new tool for the molecular characterization of pathological fluid collections [21]. Technically, the DWI sequences are constructed by acquiring T2-based images at different b-values, through diffusion-sensitizing gradients turned on at various strengths [22]. These b-values reflect the strength and time of the gradients employed to generate such diffusion-weighted images. Subsequently, the diffusion effects are closely linked to the b value [23]. In classic pelvic examinations, ADC maps are automatically generated using all acquired b values. An adequate example is displayed in **Figure 3**. The utility of this technique in differentiating endometriomas from HCs was also investigated in several studies, with contradictory results (**Table 2**).

Overall, the studies conducted by Lee [12] and Balaban [24] showed a statistically significant difference between the ADC values measured in the two groups, while no such difference was observed in a third study conducted by Lupean [18]. Interestingly, in the studies coordinated by Balaban [24] and Lupean [18], the recorded ADC values were higher for HCs than for endometriomas, while Lee [12] obtained opposite results. It is possible that due to the short-living nature of HCs, these lesions do not have the necessary time to build up blood and degradation products, and therefore they produce have a higher motion degree of the water molecules and therefore a lesser decrease of ADC values. However, the differentiation of the two entities based on diffusion

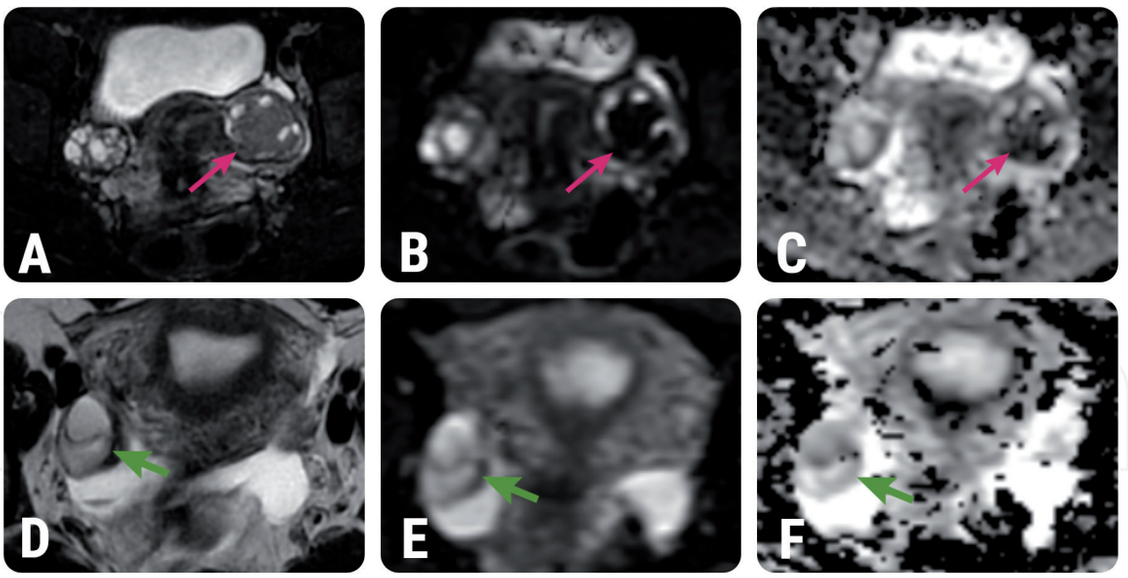

Figure 3.
(A) Axial T2 fat sat, (B) Axial DWI (b = 200), and (C) ADC map of a left-ovarian endometriotic lesion (red arrows). (D) Axial T2, (E) axial DWI, and (F) ADC map of a right-ovarian hemorrhagic cyst (green arrows). There is an obvious lower ADC signal intensity for the endometrioma (red arrow in (C)) than for the hemorrhagic cyst (green arrow in (F)).

Author	Endometriomas		HCs		p-Value	Cut-off	Se	Sp
	n	ADC	n	ADC				
Lee et al. [12]	91	1.06	21	0.73	<0.002	0.849	77.6%	76.2%
Balaban et al. [24]	12	1.84	12	2.70	<0.0001	1.54	100%	92%
Lupean et al. [18]	28	0.964	18	1.001	0.52	—	—	—

n, number of patients; HCs, hemorrhagic cysts; ADC, median ADC values expressed as number × 10^{-3} mm^2/s; cut-off, ADC cut-off value expressed as number × 10^{-3} mm^2/s; p-value, univariate analysis result; Se, sensitivity; Sp, specificity.

Table 2.
The main results that were obtained by studies that focused on the role of differentiating endometriomas from hemorrhagic cysts through apparent diffusion coefficients.

sequences seems unreliable, considering the changing nature of HCs and therefore the variable results obtained in different studies. Therefore, the MRI diffusion techniques may be less suitable for the characterization of ovarian endometriotic lesions.

4. Texture analysis

4.1 Technical considerations

Sometimes the classic imaging features of different types of adnexal lesions may be subtle or overlap, resulting in experts giving the wrong interpretation [25]. For these reasons, in most cases, a definitive diagnosis of an ovarian mass can be made only based on pathological analysis, which raises the patients' risks and healthcare costs.

It is theorized that the several micro and macroscopic histological characteristics of ovarian masses can also be reflected into the background of medical images, but their influence is too subtle to be assessed by the common visual evaluation. Textures represent the intrinsic and intuitive properties of surfaces such as roughness, granulation, and regularity. Texture analysis (TA) is an image processing method based on the extraction and analysis of image-specific parameters that reflect the pixels' distribution patterns and intensity variations [26]. Through these processes, TA provides an objective description of image content by attributing values to several

classes of texture parameters. The basic principle of image-based TA is that a pathological process that alters a tissue produces a modified signal, which will, in turn, give textural features different values from those of the normal structure [27].

The standard TA workflow consists of five steps: image segmentation, feature extraction, feature reduction, feature selection, and class prediction. Image segmentation can be performed automatically, semi-automatically, or manually. It consists of incorporating a given structure into a region of interest (ROI). Most often, researchers choose a semi-automatic technique, where a seed is defined near the center of the target lesion and the software automatically delineates the rest of the lesion based on gradient and geometry coordinates. The region or volume of interest could be delineated as a two or three-dimensional structure, the latter being able to provide more information at the cost of higher definition times [19]. However, it was proven that the latter reduces operator variability associated with multislice/volumetric analysis [20]. Therefore, it remains debatable which form will be best suited for clinical implementation. The TA parameters' extraction is performed automatically in almost all available software. The user can, however, adjust several settings regarding the parameters' computation methods (such as the number of bits/pixel and inter-pixel distances). Most software solutions allow the extraction of a large number of texture features (parameters), which can be more difficult to process by researchers that are not familiar with statistical analysis. Therefore, in order to identify the parameters that are most suited to discriminate between groups, several reduction techniques can be available (such as Fisher, Mutual Information, and the probability of classification error and average correlation coefficients) [21]. The number of parameters can be furtherly reduced by univariate analysis (typically the Mann-Whitney U test), or this analysis could be used as the only reduction and selection technique [28]. Class prediction (or the ability of previously-selected texture parameters to distinguish between vectors belonging to different pre-defined groups) can be performed statistically through the receiver operating characteristic analysis or by the use of classifiers (such as k-nearest neighbors algorithm or artificial neural networks) [29]. One of the most often used software for TA-related medical imaging research remains MaZda, which provides build-in functions for feature selection and class prediction [30]. A typical workflow for feature extraction in MaZda is displayed in **Figure 4**.

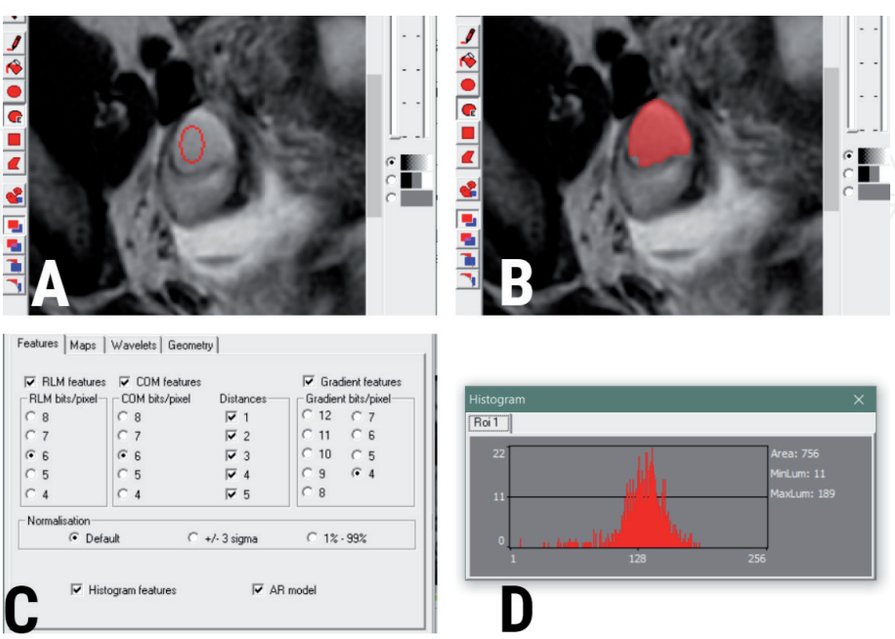

Figure 4.
Workflow within the MaZda software for extracting texture parameters from a T2-weighted MRI image of a patient with an ovarian hemorrhagic cyst. (A) The region of interest (ROI) seed placed by the researcher (red ellipse) and (B) the ROI that was automatically defined by the software. Before feature extraction, parameter settings can be adjusted (C). Histogram representation based on the parameters extracted from the lesion (D).

Texture parameter	Role
Wavelet energy	Measures local variations of pixel intensity [31]
Entropy	Measures the degree of the disorder among pixels within an image; is inversely correlated with uniformity [32]
Sum entropy	Measures the complexity of pixel values distribution [33]
Angular second moment	Directly proportional with the gray level distribution (image uniformity) [34]
Variance	Inversely proportional with image uniformity [35]

Table 3.
A brief description of the MRI-based texture parameters that showed statistically significant results when comparing endometriomas to HCs, based on the study conducted by Lupean et al. [25].

4.2 MRI-based TA for the diagnosis of endometriomas

One study [25] analyzed the texture parameters' ability to distinguish endometriomas from HCs. This study [25] extracted texture features from the internal content of these lesions as seen on T2W. Fourteen parameters showed statistically significant results when comparing the two entities: two variations of the wavelet energy, seven variations of entropy, three of the angular second moment, one of the sum entropy, and the histogram's variance (**Table 3**). Their combined ability was able to differentiate the two entities with a sensitivity of 100% [95% confidence interval (95% CI), 85.8–100%] and a specificity of 100% (95% CI, 71.5–100%).

HCs displayed lower values of wavelet energy, most likely because their content is more homogeneous, resulting in lower signal variation rates [25]. Also, these lesions expressed lower values of the entropy and sum entropy parameters, probably because they do not contain such diverse cell populations and heterogeneous biochemical components compared to endometriomas [36]. Endometriomas on the other hand showed lower values of the angular second moment and higher value of the variance parameter, indicating a lesser uniform content for these lesions (**Figure 5**). These parameters were considered reflections of the heterogeneous content of endometriomas, which otherwise could not be assessed by the usual examinations of the MRI images [25].

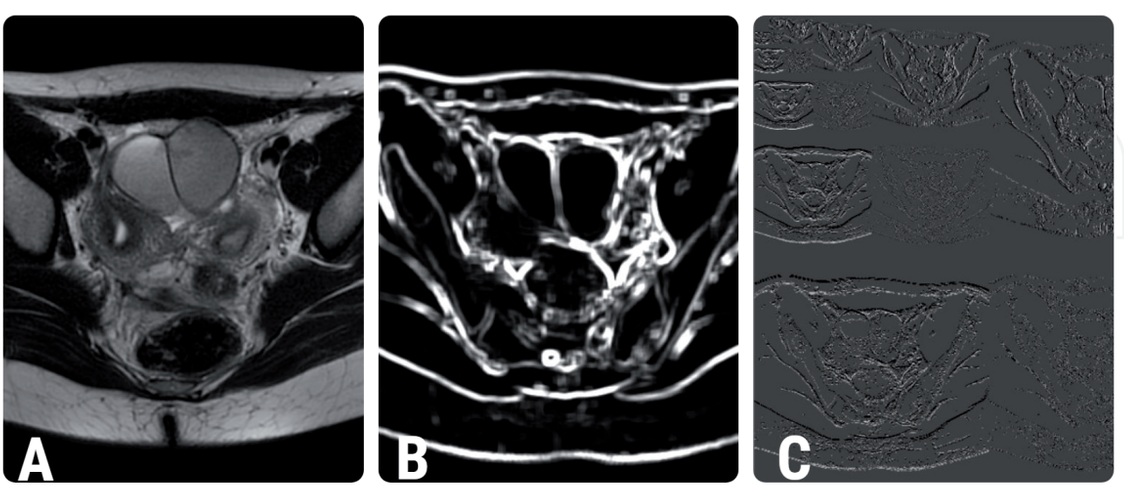

Figure 5.
(A) T2-weighted image of a patient with histologically-proven endometriomas. The texture maps show the distribution of the variance (B) and wavelet energy (C) parameters.

4.3 Ultrasound-based TA for the diagnosis of endometriomas

The ultrasound (US) appearance of endometriomas mainly depends on the time-lapse of blood degradation [37]. Most often, these lesions express a "ground

Author	Year	Se	Sp
Patel et al. [38]	1999	30–95%	49–90%
Mais et al. [39]	1993	84%	90%
Alcázar et al. [40]	1997	88.9%	91%
Van Holsbeke et al. [41]	2010	73%	94%

Table 4.
Studies that evaluated the diagnostic utility of the "ground glass" appearance of endometriomas.

glass" appearance, a feature to which different degrees of accuracy have been attributed over time (**Table 4**).

In practice, the grayscale US of endometriomas and HCs can be very similar, both lesions showing characteristics of different stages of blood degradation, making the distinction difficult [42]. A study [43] showed that 20 texture parameters that were extracted from the US of greyscale images showed statistically significant results when distinguishing endometriomas from HCs. Their combined ability was able to differentiate between the two entities with 100% (95% CI, 88.4–100%) sensitivity and 100% (95% CI, 75.3–100%) [43]. Three parameters were proved to be independent predictors of endometriomas (difference variance, contrast, and the 10th percentile) (**Figure 6**) [43]. The difference of variance parameter measures the variance of the difference of gray level values (reflecting the randomness within an image) [44]. The contrast parameter shows the local variations present in an image, expressing higher values when an image contains a large number of pixels with different gray level values [45]. The study [43] showed that both of these parameters held higher values for HCs than for endometriomas. On the other hand, the 10th percentile showed higher values for endometriomas than for HCs, which signifies that 10% of the pixels within images were distributed under higher values for endometriomas than for HOCs [43]. Even though endometriomas were expected to have a higher degree of echogenic randomness due to a large number of contained elements, HCs displayed higher values for the parameters that mirror these characteristics [43]. This finding is consistent with the literature, which suggests

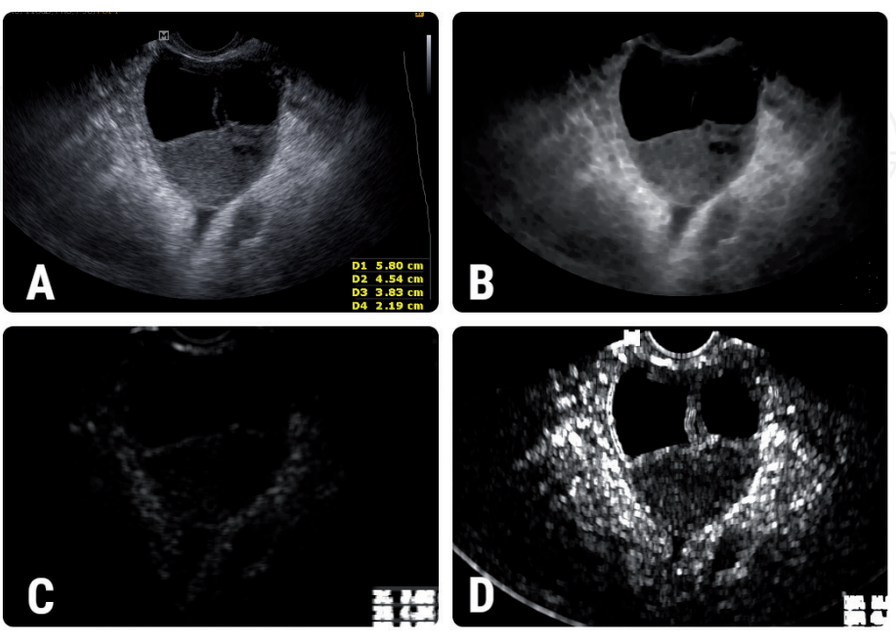

Figure 6.
(A) T2-weighted image of a patient with histologically-proven endometrioma. The texture maps show the distribution of the (B) 10th percentile, (C) contrast, and (D) difference variance parameters.

that HOCs have more complicated and heterogeneous content on TVUS (since they express tiny linear strands and retraction clots more frequently) [46].

5. Conclusion

The current imaging diagnosis of endometriomas encounters several limitations, including a similar appearance to other hemorrhagic adnexal lesions and the subjective nature of the imaging signs considered specific to this disease. Quantitative imaging methods (such as MRI SI measurements and TA) can improve the diagnostic confidence of endometriomas, but the studies validating these methods are certainly required.

Conflict of interest

The authors declare no conflict of interest.

Author details

Paul-Andrei Ștefan[1,2,3], Roxana-Adelina Lupean[1,4*] and Dietmar Tamandl[3]

1 "Iuliu Haţieganu" University of Medicine and Pharmacy, Cluj-Napoca, Romania

2 Radiology and Imaging Department, Cluj County Emergency Clinical Hospital, Cluj-Napoca, Romania

3 Department of Biomedical Imaging and Image-Guided Therapy, Medical University of Vienna, General Hospital of Vienna (AKH), Wien, Österreich

4 Obstetrics and Gynecology Clinic "Dominic Stanca", Cluj County Emergency Hospital, Cluj-Napoca, Romania

*Address all correspondence to: roxanalupean92@gmail.com

References

[1] Siegelman ES, Oliver ER. MR imaging of endometriosis: Ten imaging pearls. Radiographics. 2012;**32**:1675-1691. DOI: 10.1148/rg.326125518

[2] Van den Bosch T, Van Schoubroeck D. Ultrasound diagnosis of endometriosis and adenomyosis: State of the art. Best Practice & Research. Clinical Obstetrics & Gynaecology. 2018;**51**:16-24. DOI: 10.1016/j.bpobgyn.2018.01.013

[3] Kinkel K, Frei KA, Balleyguier C, Chapron C. Diagnosis of endometriosis with imaging: A review. European Radiology. 2006;**16**:285-298. DOI: 10.1007/s00330-005-2882-y

[4] Robinson AJ, Rombauts L, Ades A, Leong K, Paul E, Piessens S. Poor sensitivity of transvaginal ultrasound markers in diagnosis of superficial endometriosis of the uterosacral ligaments. Journal of Endometriosis and Pelvic Pain Disorders. 2018;**10**:10-17. DOI: 10.1177/2284026518767259

[5] Kim H-J, Lee S-Y, Shin YR, Park CS, Kim K. The value of diffusion-weighted imaging in the differential diagnosis of ovarian lesions: A meta-analysis. PLoS One. 2016;**11**:e0149465. DOI: 10.1371/journal.pone.0149465

[6] Tanase Y, Kawaguchi R, Takahama J, Kobayashi H. Factors that differentiate between endometriosis-associated ovarian cancer and benign ovarian endometriosis with mural nodules. Magnetic Resonance in Medical Sciences. 2018;**17**:231-237. DOI: 10.2463/mrms.mp.2016-0149

[7] Foti PV, Attinà G, Spadola S, Caltabiano R, Farina R, Palmucci S, et al. MR imaging of ovarian masses: Classification and differential diagnosis. Insights Into Imaging. 2016;7:21-41. DOI: 10.1007/s13244-015-0455-4

[8] Glastonbury CM. The Shading Sign. Radiology. 2002;**224**:199-201. DOI: 10.1148/radiol.2241010361

[9] Siegelman ES, Outwater EK. Tissue characterization in the female pelvis by means of MR imaging. Radiology. 1999;**212**:5-18. DOI: 10.1148/radiology.212.1.r99jl455

[10] Togashi K, Nishimura K, Kimura I, Tsuda Y, Yamashita K, Shibata T, et al. Endometrial cysts: Diagnosis with MR imaging. Radiology. 1991;**180**:73-78. DOI: 10.1148/radiology.180.1.2052726

[11] Outwater E, Schiebler ML, Owen RS, Schnall MD. Characterization of hemorrhagic adnexal lesions with MR imaging: Blinded reader study. Radiology. 1993;**186**:489-494. DOI: 10.1148/radiology.186.2.8421756

[12] Lee NK, Kim S, Kim KH, Suh DS, Kim TU, Han GJ, et al. Diffusion-weighted magnetic resonance imaging in the differentiation of endometriomas from hemorrhagic cysts in the ovary. Acta Radiologica. 2016;**57**:998-1005. DOI: 10.1177/0284185115609805

[13] Corwin MT, Gerscovich EO, Lamba R, Wilson M, McGahan JP. Differentiation of ovarian endometriomas from hemorrhagic cysts at MR imaging: Utility of the T2 dark spot sign. Radiology. 2014;**271**:126-132. DOI: 10.1148/radiol.13131394

[14] Kanso HN, Hachem K, Aoun NJ, Haddad-Zebouni S, Klein-Tomb L, Atallah D, et al. Variable MR findings in ovarian functional hemorrhagic cysts. Journal of Magnetic Resonance Imaging. 2006;**24**:356-361. DOI: 10.1002/jmri.20640

[15] Dias JL, Veloso Gomes F, Lucas R, Cunha TM. The shading sign: Is it exclusive of endometriomas? Abdominal Imaging. 2015;**40**:2566-2572. DOI: 10.1007/s00261-015-0465-1

[16] Sugimura K, Okizuka H, Imaoka I, Kaji Y, Takahashi K, Kitao M, et al. Pelvic endometriosis: Detection and diagnosis with chemical shift MR imaging. Radiology. 1993;**188**:435-438. DOI: 10.1148/radiology.188.2.8327693

[17] Scoutt LM, McCarthy SM, Lange R, Bourque A, Schwartz PE. MR evaluation of clinically suspected adnexal masses. Journal of Computer Assisted Tomography. 1994;**18**:609-618. DOI: 10.1097/00004728-199407000-00019

[18] Lupean R-A, Ștefan P-A, Lebovici A, Csutak C, Rusu GM, Mihu CM. Differentiation of endometriomas from hemorrhagic cysts at magnetic resonance: The role of quantitative signal intensity measurements. Current Medical Imaging. 2021;**17**:524-531. DOI: 10.2174/1573405616999201027211132

[19] Agostinho L, Horta M, Salvador JC, Cunha TM. Benign ovarian lesions with restricted diffusion. Radiologia Brasileira. 2019;**52**:106-111. DOI: 10.1590/0100-3984.2018.0078

[20] Lupean R-A, Ștefan P-A, Feier DS, Csutak C, Ganeshan B, Lebovici A, et al. Radiomic analysis of MRI images is instrumental to the stratification of ovarian cysts. Journal of Personalized Medicine. 2020;**10**:E127. DOI: 10.3390/jpm10030127

[21] Mayerhoefer ME, Breitenseher M, Amann G, Dominkus M. Are signal intensity and homogeneity useful parameters for distinguishing between benign and malignant soft tissue masses on MR images? Objective evaluation by means of texture analysis. Magnetic Resonance Imaging. 2008;**26**:1316-1322. DOI: 10.1016/j.mri.2008.02.013

[22] DWI. Questions and Answers in MRI. Availble from: http://mriquestions.com/making-a-dw-image.html [Accessed: November 3, 2021]

[23] b-value diffusion. Questions and Answers in MRI. Available from: http://mriquestions.com/what-is-the-b-value.html [Accessed: November 3, 2021]

[24] Balaban M, Idilman IS, Toprak H, Unal O, Ipek A, Kocakoc E. The utility of diffusion-weighted magnetic resonance imaging in differentiation of endometriomas from hemorrhagic ovarian cysts. Clinical Imaging. 2015;**39**:830-833. DOI: 10.1016/j.clinimag.2015.05.003

[25] Lupean R-A, Ștefan P-A, Csutak C, Lebovici A, Măluțan AM, Buiga R, et al. Differentiation of endometriomas from ovarian hemorrhagic cysts at magnetic resonance: The role of texture analysis. Medicina (Kaunas, Lithuania). 2020;**56**:E487. DOI: 10.3390/medicina56100487

[26] Larroza A, Bodí V, Moratal D. Texture analysis in magnetic resonance imaging: Review and considerations for future applications. In: Assessment of Cellular and Organ Function and Dysfunction Using Direct and Derived MRI Methodologies. London, UK: InTechOpen; 2016

[27] Morris DT. An evaluation of the use of texture measurements for the tissue characterisation of ultrasonic images of in vivo human placentae. Ultrasound in Medicine & Biology. 1988;**14**:387-395. DOI: 10.1016/0301-5629(88)90074-9

[28] Csutak C, Ștefan P-A, Lenghel LM, Moroșanu CO, Lupean R-A, Șimonca L, et al. Differentiating high-grade gliomas from brain metastases at magnetic resonance: The role of texture analysis of the peritumoral zone. Brain Sciences. 2020;**10**:E638. DOI: 10.3390/brainsci10090638

[29] Stefan P-A, Puscas ME, Csuak C, Lebovici A, Petresc B, Lupean R, et al. The utility of texture-based classification of different types of ascites on magnetic resonance. Journal of BUON. 2020;**25**:1237-1244

[30] Strzelecki M, Szczypinski P, Materka A, Klepaczko A. A software tool for automatic classification and segmentation of 2D/3D medical images. Nuclear Instruments and Methods in Physics Research A. 2013;**702**:137-140

[31] Livens S. Wavelets for texture analysis, an overview. In: Proceedings of the 6th International Conference on Image Processing and its Applications. Dublin, Ireland: IET - Institution of Engineering and Technology; 14-17 July 1997. pp. 581-585

[32] Zhao H, Feng X, Chen Y, Zhao S, Xiao P. Entropy-based texture analysis and feature extraction of urban street trees in the spatial frequency domain. In: Proceedings of the Sixth International Symposium on Multispectral Image Processing and Pattern Recognition. Yichang, China: Society of Photo-Optical Instrumentation Engineers (SPIE); 30 October–1 November 2009. Vol. 7495. p. 749513

[33] Jernigan ME, D'Astous F. Entropy-based texture analysis in the spatial frequency domain. IEEE Transactions on Pattern Analysis and Machine Intelligence. 1984;**6**:237-243

[34] Texture Analysis Using Co-Occurrence Matrix. Available from: https://www.massey.ac.nz/~{}mjjohnso/notes/59731/presentations/texture.pdf [Accessed: August 12, 2021]

[35] Writh A. Texture Analysis. Available from: http://www.cyto.purdue.edu/cdroms/micro2/content/education/wirth06.pdf [Accessed: August 13, 2021]

[36] Bibbo M, Wood MD, Fitzpatrick BT. Peritoneal washings and ovary. In: Wilbur D, editor. Comprehensive Cyto-Pathology E-Book. Amsterdam, The Netherlands: Elsevier Health Sciences; 2014. pp. 291-301

[37] Collins BG, Ankola A, Gola S, McGillen KL. Transvaginal US of endometriosis: Looking beyond the endometrioma with a dedicated protocol. Radiographics. 2019;**39**:1549-1568. DOI: 10.1148/rg.2019190045

[38] Patel MD, Feldstein VA, Chen DC, Lipson SD, Filly RA. Endometriomas: Diagnostic performance of US. Radiology. 1999;**210**:739-745. DOI: 10.1148/radiology.210.3.r99fe61739

[39] Mais V, Guerriero S, Ajossa S, Angiolucci M, Paoletti AM, Melis GB. The efficiency of transvaginal ultrasonography in the diagnosis of endometrioma. Fertility and Sterility. 1993;**60**:776-780. DOI: 10.1016/S0015-0282(16)56275-X

[40] Alcázar JL, Laparte C, Jurado M, Lopez-Garcia G. The role of transvaginal ultrasonography combined with color velocity imaging and pulsed Doppler in the diagnosis of endometrioma. Fertility and Sterility. 1997;**67**:487-491. DOI: 10.1016/S0015-0282(97)80074-X

[41] Van Holsbeke C, Van Calster B, Guerriero S, Savelli L, Paladini D, Lissoni AA, et al. Endometriomas: Their ultrasound characteristics. Ultrasound in Obstetrics & Gynecology. 2010;**35**:730-740. DOI: 10.1002/uog.7668

[42] Batur A, Yavuz A, Ozgokce M, Bora A, Bulut MD, Arslan H, et al. The utility of ultrasound elastography in differentiation of endometriomas and hemorrhagic ovarian cysts. Journal of Medical Ultrasonics. 2016;**43**:395-400. DOI: 10.1007/s10396-016-0701-5

[43] Ștefan R-A, Ștefan P-A, Mihu CM, Csutak C, Melincovici CS, Crivii CB, et al. Ultrasonography in the differentiation of endometriomas from hemorrhagic ovarian cysts: The role of texture analysis. Journal of Personalized Medicine. 2021;**11**:611. DOI: 10.3390/jpm11070611

[44] Durgamahanthi V, Christaline JA, Edward AS. GLCM and GLRLM based texture analysis: Application to brain cancer diagnosis using histopathology images. In: ; Dash SS, Das S, Panigrahi BK. Intelligent Computing and Applications. Singapore: Springer; 2020; pp. 691-706

[45] Biomedical Informatics 260. Computational Feature Extraction: Texture Features Lecture 6 David Paik. Available from: https://docplayer.net/188454072-Biomedical-informatics-260-computational-feature-extraction-texture-features-lecture-6-david-paik-phd-spring-2019.html [Accessed: May 26, 2021]

[46] Rezvani M. Nonneoplastic ovarian lesions: Endometrioma. In: Shaaban AM, Menias CO, Tubay MS, editors. Diagnostic Imaging: Gynecology. 2nd ed. Amsterdam, The Netherlands: Elsevier; 2015. p. 190